



Harmonic injection locking of high-power mid-infrared quantum cascade lasers

F. WANG, S. SLIVKEN, AND M. RAZEGHI*

Center for Quantum Devices, Department of Electrical Engineering and Computer Science, Northwestern University, Evanston, Illinois 60208, USA

*Corresponding author: razeghi@northwestern.edu

Received 24 February 2021; revised 1 April 2021; accepted 3 April 2021; posted 5 April 2021 (Doc. ID 423573); published 27 May 2021

High-power, high-speed quantum cascade lasers (QCLs) with stable emission in the mid-infrared regime are of great importance for applications in metrology, telecommunication, and fundamental tests of physics. Owing to the intersubband transition, the unique ultrafast gain recovery time of the QCL with picosecond dynamics is expected to overcome the modulation limit of classical semiconductor lasers and bring a revolution for the next generation of ultrahigh-speed optical communication. Therefore, harmonic injection locking, offering the possibility to fast modulate and greatly stabilize the laser emission beyond the rate limited by cavity length, is inherently adapted to QCLs. In this work, we demonstrate for the first time the harmonic injection locking of a mid-infrared QCL with an output power over 1 W in continuous-wave operation at 288 K. Compared with an unlocked laser, the intermode spacing fluctuation of an injection-locked QCL can be considerably reduced by a factor above 1×10^3 , which permits the realization of an ultrastable mid-infrared semiconductor laser with high phase coherence and frequency purity. Despite temperature change, this fluctuation can be still stabilized to hertz level by a microwave modulation up to ~ 18 GHz. These results open up the prospect of the applications of mid-infrared QCL technology for frequency comb engineering, metrology, and the next-generation ultrahigh-speed telecommunication. It may also stimulate new schemes for exploring ultrafast mid-infrared pulse generation in QCLs. © 2021 Chinese Laser Press

<https://doi.org/10.1364/PRJ.423573>

1. INTRODUCTION

Injection locking was originally used to build a powerful and spectrally pure laser in the master oscillator power amplifier (MOPA) architecture, where a well-controlled low-power frequency stable laser is injected into a powerful but spectrally broad laser [1–3]. Then the spectral purity of the master laser can be transferred to the powerful slave laser. This technique shows great advantages for the amplification and stabilization of a single-mode laser. However, for a multimode laser it is challenging, as it requires locking a few or even hundreds of longitudinal modes individually. Electrical injection locking is, therefore, developed to achieve the same goal through locking the intermode spacing, instead of longitudinal modes directly, of a semiconductor laser by applying a microwave signal that is resonant with its round-trip frequency. This approach has enabled active and hybrid mode locking of interband semiconductor lasers [4–6].

Harmonic injection locking is routinely used in the visible and near-infrared range to generate multiple light pulses within the photon round-trip time of a laser cavity. This provides the possibility to get high-repetition-rate laser systems, which is of particular interest in high-bit-rate optical communication [7],

photonic analogue-to-digital conversion [8], multiphoton imaging [9], and astronomical frequency comb generation [10]. Owing to the intersubband transition [11,12], the unique ultrafast gain recovery time of a quantum cascade laser (QCL) with picosecond relaxation dynamics that is not present in other laser systems is expected to overcome the limit of response to direct high-speed gain/loss modulation in classical semiconductor lasers. Therefore, harmonic, especially high-order harmonic, injection locking is inherently adapted to QCLs [13], which can potentially open up the prospect of applications of high-power, high-speed semiconductor lasers in the mid-infrared range for frequency comb engineering, metrology, and the next-generation ultrahigh-speed telecommunication. This is in strong contrast to the traditional opinions that have considered these ultrafast dynamics of QCLs as an inhibitor and a bottleneck to the widespread use of these unipolar semiconductor lasers. Besides, high-order harmonic injection locking with modulation speed faster or equivalent to the gain recovery time of QCL might also provide the potential to generate ultrafast mid-infrared light pulses with extremely high repetition rate far beyond the current state of the art in semiconductor lasers. This has been one of the main challenges in

the QCL community for many years despite some recently reported results [14,15].

Although injection locking of mid-infrared QCLs has been demonstrated, it was only applied to very low output power (<200 mW) and very low operating temperature (<80 K) devices [16,17], which strongly limits its broad-ranging applications across the domains of fundamental physics, high-precision metrology, and wireless communication. Harmonic injection-locked QCLs have also been demonstrated recently in the terahertz (THz) range, but their output power is extremely low ($\sim 10 \mu\text{W}$), even at liquid helium temperature (10 K) [13]. To date, no demonstration of harmonic injection locking of QCL has been done in the mid-infrared regime. In this work, we demonstrate for the first time to our knowledge the injection locking and harmonic injection locking of a mid-infrared QCL at $\lambda \approx 8.2 \mu\text{m}$ with an output power over 1 W in continuous-wave (CW) operation at 288 K. We also examined the experimental results in the theoretical framework of injection locking. They are well in agreement with each other. Varying the operating temperature of the injection-locked QCL within 1°C , its intermode spacing fluctuation can be still stabilized to hertz level by the external microwave modulation up to $\sim 18 \text{ GHz}$.

2. QCL AND EXPERIMENTAL SETUP

In this work, the QCL structure is a high-efficiency active region design at $\lambda \approx 8.2 \mu\text{m}$, which utilizes a strain-balanced $\text{Al}_{0.64}\text{In}_{0.36}\text{As}/\text{In}_{0.59}\text{Ga}_{0.41}\text{As}$ material system based on an n-InP substrate [18,19]. Strong coupling between the upper lasing level and injector levels has been engineered to increase gain bandwidth and injection efficiency. To achieve harmonic injection locking, the nonlinearity of the QCL is also engineered in the miniband to enhance the four-wave-mixing process and obtain strong harmonic electrical beating [18–20]. The growth was performed using gas-source molecular beam epitaxy (MBE), and the wafer was processed into a buried ridge waveguide with a ridge width of $\sim 8 \mu\text{m}$ using standard photolithography. The laser bar was cleaved into a 5 mm long cavity and epilayer-down bonded on a diamond submount for efficient heat dissipation. In order to extract high power from the laser cavity, its back facet was high-reflection (HR) coated using $\text{Y}_2\text{O}_3/\text{Au}/\text{Ti}$, and the front one was antireflection (AR) coated using 800 nm thick Y_2O_3 as shown in Fig. 1(a). The light-current-voltage (LIV) characteristics of this device are shown

in Fig. 1(b). At 288 K, laser threshold is observed at 0.56 A ($1.41 \text{ kA}/\text{cm}^2$). Maximum outcoupling power is $>2 \text{ W}$ in CW operation. Its slope efficiency (SE) and wall plug efficiency (WPE) were $\sim 2.56 \text{ W}/\text{A}$ and $\sim 14\%$, respectively. A thermoelectric cooler stage was used to carry away the thermal accumulation.

The experimental setup is schematically illustrated in Fig. 2. The high-performance QCL is biased at 1165 mA using a low-noise current source (Wavelength Electronics QCL2000). The QCL emission is coupled into a quantum well infrared photo-detector (QWIP) for beat note measurements. The tunable RF signal is first amplified and then injected into the QCL through a high-speed, low-loss RF waveguide similar to Ref. [21]. This coplanar waveguide, capable of transmitting signals from DC up to $>100 \text{ GHz}$, significantly lowers the connection losses and permits efficient RF power injection for high-power QCL locking.

3. INJECTION LOCKING

Prior to investigating harmonic injection locking, we firstly demonstrate the fundamental injection locking of a mid-infrared QCL with watt-level output power in CW operation at high temperature (288 K). In a QCL system, the electrical beating of the quasi-equally spaced Fabry–Perot modes (f_n) will generate a beat note signal that can be expressed as $S(f) = \sum S_i(f_{n+1} - f_n)$. The bandwidth of the beat note depends on the fluctuation of the intermode spacings of the laser. As shown in Figs. 3(a) and 3(b), the beat note of the QCL used in this paper is located at $f_{\text{beatnote}} \approx 8964 \text{ MHz}$ when the laser is biased at 1164 mA. Similar to optical injection locking, by injecting an RF signal (f_{RF}) that is resonant with the beat note frequency (f_{beatnote}) into the QCL system, the spectral purity and stability of the low-noise external RF signal can be transferred to the beat note through light–matter interaction. From the complex amplitude evolution of the RF field in the system, the injection locking can be described using the following equation [22]:

$$\frac{d\varphi}{dt} = \omega_{\text{RF}} - \Delta\omega - \omega_L \sin \varphi. \quad (1)$$

In Eq. (1), φ is the phase difference between the injected RF signal and the beat note signal, ω_{RF} is the angular frequency of the RF signal, $\Delta\omega$ is the angular frequency of the beat note, and

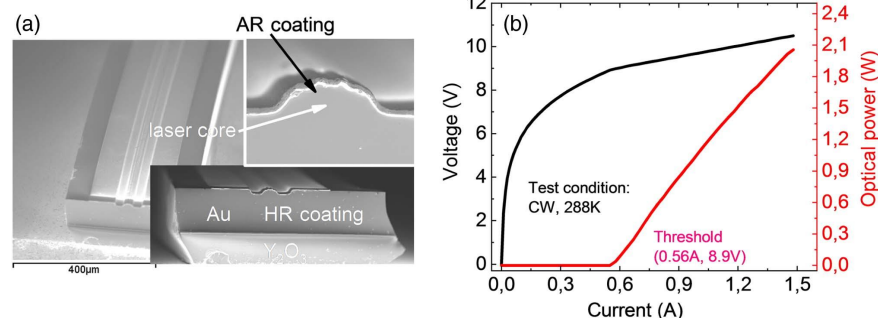


Fig. 1. (a) The scanning electron microscopy (SEM) image of the QCL device and its HR coated and AR coated facets. (b) Light-current-voltage (LIV) curves of this QCL.

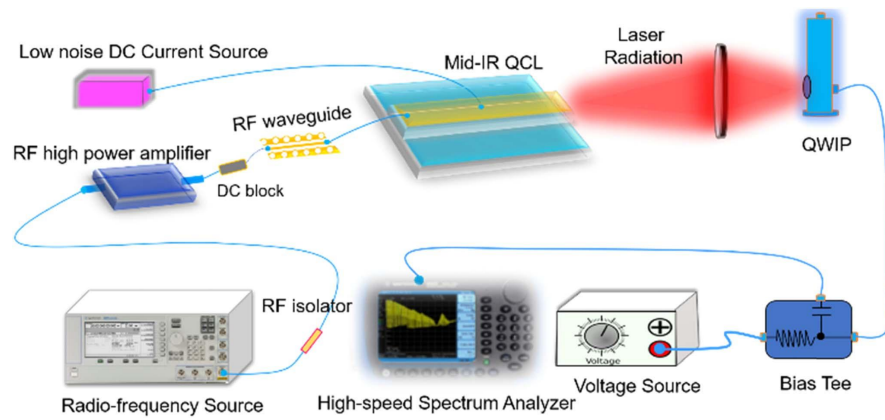


Fig. 2. Experimental setup. The mid-infrared QCL is biased by a low-noise DC current source. Laser emission is coupled into a quantum well infrared photodetector (QWIP). The high frequency components of the photocurrents are coupled into a spectrum analyzer. RF waves are generated by a RF generator and amplified by a high-power amplifier. The RF signal is injected into the QCL through a high-speed RF waveguide from near the back facet of the QCL.

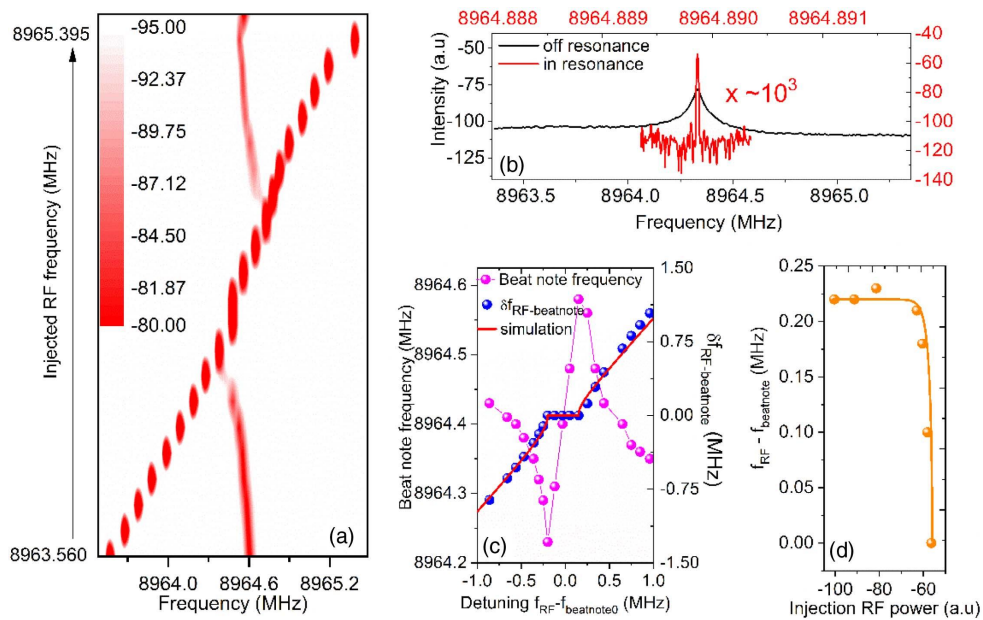


Fig. 3. (a) The evolution of the beat note (continuous branch) of the QCL as a function of the injected RF frequency (discrete branch) (each injected RF frequency can be found in the x axis). (b) The beat note linewidth of the QCL at off-resonance and resonance conditions, respectively. (c) Magenta: the beat note frequency as a function of the detuning δ between RF frequency f_{RF} and the beat note without RF injection Δf_0 . Blue: the frequency difference $\delta f_{\text{RF-beatnote}}$ between RF and beat note as a function of detuning δ . (d) The power dependence experiment (ball) and simulation (curve) of the frequency difference $\delta f_{\text{RF-beatnote}}$.

$\omega_L \sim (P_{\text{inj}}/P_0)^{1/2}$ is the locking range, determined by the injected RF power P_{inj} and the intracavity laser power P_0 . When $|\omega_{\text{RF}} - \Delta\omega| < \omega_L$, Eq. (1) has steady-state solution: $\sin \varphi = (\omega_{\text{RF}} - \Delta\omega)/\omega_L$. In this case, the beat note is resonant with the injected RF signal. When $|\omega_{\text{RF}} - \Delta\omega| > \omega_L$, Eq. (1) can no longer have any steady-state solution, falling out of the locking range.

With an injection current of 1165 mA, the output power of the QCL is over 1 W in CW operation at 288 K as shown in Fig. 1(b). At this operating condition, we inject an RF frequency into the QCL system and increase it step by step from 8963.560 to 8965.395 MHz. Intuitively, the beat note

evolution process can be divided into three regimes as shown in Fig. 3(a). (i) Within [8963.560 MHz, 8964.395 MHz], the beat note is pulled toward the RF frequency from 8964.615 to 8964.395 MHz. This is out of injection locking. (ii) From 8964.395 to 8964.740 MHz, the beat note is in resonance with the RF signal, and their frequencies are clamped to each other ($f_{\text{beatnote}} = f_{\text{RF}}$). (iii) From 8964.740 to 8965.395 MHz, the laser goes beyond the resonance regime again, and the beat note gradually moves away from the RF signal. When the RF signal is off-resonance with the laser system, the linewidth (FWHM) of the beat note is on the order of 90 kHz. While they are in resonance, the beat note linewidth dramatically drops down to

hertz level (20 Hz) as shown in Fig. 3(b). This phenomenon revealed that the mid-infrared QCL is greatly stabilized, and its intermode spacing fluctuation is decreased by a factor above 1×10^3 .

Figure 3(c) (magenta) shows the beat note of the QCL as a function of detuning $\delta = f_{\text{RF}} - f_{\text{beatnote0}}$ between RF signal and initial beat note. Equivalently, Fig. 3(c) (blue) shows the frequency difference $\delta f_{\text{RF-beatnote}}$ between RF and beat note as a function of δ . The three physical processes discussed above can be clearly identified in both of the two curves. A resonant locking range of $f_L = \omega_L/2\pi = 0.35$ MHz can be extracted. In particular, the anharmonic nature of the frequency breathing $\delta f_{\text{RF-beatnote}}$ can be observed slightly beyond the resonant region. From Eq. (1), the $\delta f_{\text{RF-beatnote}}$ is deduced to be the following:

$$\delta f_{\text{RF-beatnote}} = \frac{1}{2\pi} \sqrt{(\omega_{\text{RF}} - \Delta\omega_0)^2 - \omega_L^2}. \quad (2)$$

In Eq. (2), $\Delta\omega_0$ is the angular frequency of the beat note without RF signal injection. When $|\omega_{\text{RF}} - \Delta\omega_0| < \omega_L$, $\delta f_{\text{RF-beatnote}}$ is a pure imaginary number, corresponding to the resonant interaction between RF and laser system. The real part of $\delta f_{\text{RF-beatnote}}$ is equal to zero, indicating that their frequencies are clamped. When $|\omega_{\text{RF}} - \Delta\omega_0| > \omega_L$, $\delta f_{\text{RF-beatnote}}$ is a real number and shows anharmonic behavior versus detuning δ . While $|\omega_{\text{RF}} - \Delta\omega_0| \gg \omega_L$, $\delta f_{\text{RF-beatnote}}$ is proportional to δ . As shown in Fig. 3(c) (red), the calculation based on Eq. (2) is well in agreement with the experimental data at resonant and negative detuning regime ($\delta < 0$). When $\delta > 0.5$ MHz, they slightly diverge from each other, probably due to the asymmetry of the intersubband structure of QCL.

Figure 3(d) shows the power dependence of $\delta f_{\text{RF-beatnote}}$. The frequency difference between the beat note and the RF is initially set to be ~ 0.22 MHz. Fixing the RF frequency and increasing its power, the beat note is gradually approaching toward the RF signal. Thereby, detuning $\delta f_{\text{RF-beatnote}}$ progressively decreases and finally becomes zero when falling in resonance. This experimental result is in agreement with the simulation in Fig. 3(d) (solid line), according to Eq. (2) and $\omega_L \sim (P_{\text{inj}}/P_0)^{1/2}$. Since our device is a high-performance QCL with an output power $P_0 > 1$ W in CW operation, the locking range is limited to ~ 0.35 MHz as can be directly observed in Figs. 3(a) and 3(c). However, the locking range can be further extended by increasing the RF power to satisfy the requirements of applications.

Figure 4 shows the resonance and off-resonance spectra of the laser emission. In these two conditions, their bandwidths are almost identical, indicating that the linewidth reduction of the beat note in resonance is due to intermode locking, instead of emission spectrum narrowing.

To study the stability of QCL emission under temperature fluctuations, the laser was held in resonance with the RF at 15.0°C, and then we gradually varied the QCL's operation temperature from 14.0°C to 18.0°C. Within $14.5^\circ\text{C} < T < 15.5^\circ\text{C}$, the beat note frequency is always clamped to the RF frequency. While beyond this range, it moved away from the RF signal as shown in Fig. 5, where the vertical branch is the RF signal and the other is the beat note evolution versus

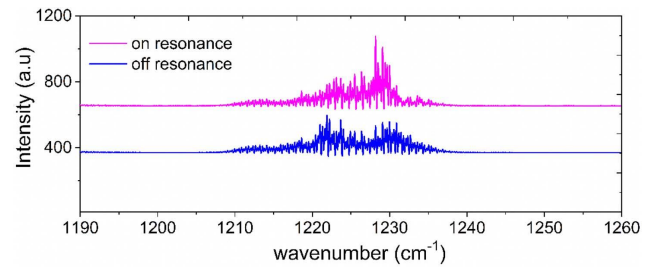


Fig. 4. Spectrum of the laser emission under resonance and off-resonance conditions.

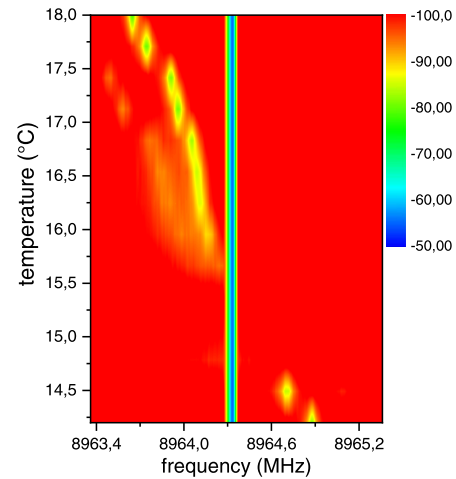


Fig. 5. Beat note evolution as a function of operating temperature. The vertical line is the injected RF signal, and the other branch is the beat note.

temperature. This result shows that the phase-stabilized QCL is capable of withstanding $\sim 1^\circ\text{C}$ temperature fluctuations without degrading its hertz-level phase coherence. Increasing the RF power, this capability of temperature fluctuation tolerance can be further extended.

4. HARMONIC INJECTION LOCKING

The beat note of a laser is the joint result of the electrical beating between any two longitudinal modes: $S(f) = \sum S(f_m - f_n)$; m, n are integers. Since a broadband QCL consists of plethora of quasi-equally spaced longitudinal modes, the beat note can be further classified by frequency: $S(f) = \sum S(f_{n+1} - f_n) + \sum S(f_{n+2} - f_n) + \sum S(f_{n+3} - f_n) + \dots$. The first term $\sum S(\Delta f = f_{n+1} - f_n)$ represents the fundamental beat note. The second term $\sum S(2\Delta f = f_{n+2} - f_n)$ is the second harmonic one, and so on. They can be simultaneously observed using a high-speed spectrum analyzer. As shown in Fig. 5(a), the first-order and second-harmonic beat notes were observed respectively at ~ 9 GHz and ~ 18 GHz. The third-order one is expected to be ~ 27 GHz, beyond the scope of our spectrum analyzer. Although fundamental injection locking is important in the stabilization of QCL emission, the high-order harmonic injection, requiring faster

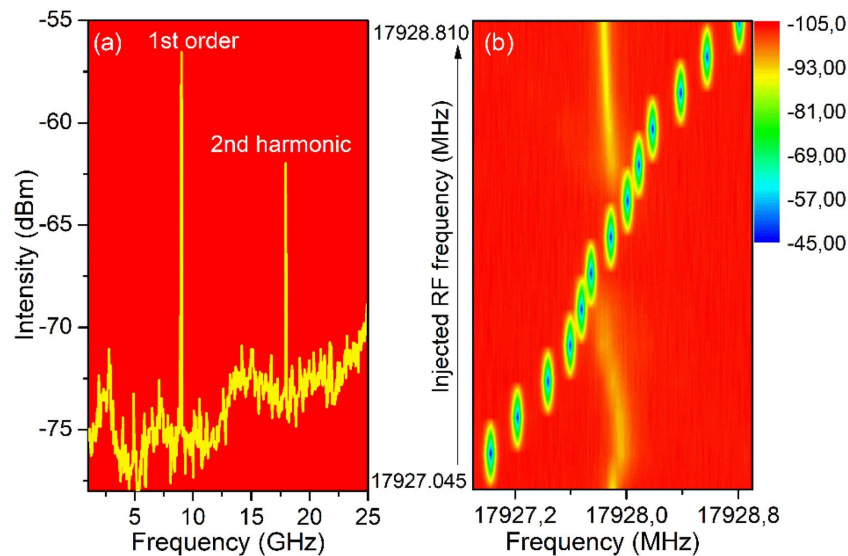


Fig. 6. (a) First-order and second-harmonic beat note. (b) The evolution of the beat note as a function of injected RF frequency. The discrete branch is the RF signal, and the continuous branch represents the beat note. (Each injected RF frequency can be found in the x axis.)

modulation, is more interesting since the unique ultrafast relaxation dynamics of a QCL on a picosecond scale are expected to enable a groundbreaking increase in the modulation speed of semiconductor lasers. This may lead to a new revolution for next-generation high-speed optical communication and signal processing. Therefore, harmonic, especially high-order harmonic, injection locking is inherently adapted to QCLs and is of great importance for future high-power, high-speed applications.

Compared with fundamental injection locking, harmonic injection locking is more difficult to achieve since (1) the harmonic electrical beating is much weaker than the fundamental one; (2) less microwave power can be injected into the laser at higher frequency. Owing to the nonlinearity enhancement in QCL design in this paper, the laser is in quasi-comb operation, and the harmonic beat note signal is still quite strong as shown in Fig. 6(a). This offers the possibility to demonstrate for the first time the second-harmonic injection locking of a mid-infrared QCL. The operating conditions of this laser are exactly the same as the ones used in the fundamental injection locking ($I = 1165$ mA, $T = 288$ K, $P_0 > 1$ W). As shown in Fig. 6(b), an RF signal (discrete) was injected into the QCL, and its frequency was gradually increased from 17927.045 to 17928.810 MHz. The second-harmonic beat note undergoes a similar process as the fundamental one. Within [17927.045 MHz, 17927.655 MHz], the second-harmonic beat note is pulled toward the RF frequency from 17927.885 to 17927.735 MHz. In this regime, the laser is out of locking. From 17927.725 to 17927.990 MHz, the second-harmonic beat note is in resonance with the injected RF signal, and their frequencies are clamped to each other ($f_{\text{beatnote}} = f_{\text{RF}}$). From 17928.065 to 17928.790 MHz, the laser goes beyond the resonance regime again, and the second-harmonic beat note gradually moves away from the RF signal. Similar to the fundamental injection locking, when the RF signal is off-resonance with the second-harmonic frequency

of the QCL, the linewidth (FWHM) of the beat note is at the order of tens of kilohertz to megahertz. While they are in resonance, the beat note linewidth dramatically drops down to hertz level despite a high output power over 1 W in CW operation. Owing to the reduced electrical beating strength as shown in Fig. 6(a), a slightly narrower locking range of ~ 0.265 MHz was obtained under the same injection RF power. This second-harmonic injection locking also exhibits a highly stable emission under a temperature fluctuation of $\sim 0.5^\circ\text{C}$. Using a faster spectrum analyzer and RF source, the third-order, fourth-order, fifth-order, ..., beat note may be observed with a distinct possibility.

Although the picosecond gain recovery time of a QCL is expected to bring high-speed applications that are out the reach of interband semiconductor lasers, it also brings difficulties and challenges to generate ultrashort light pulses via active mode locking of mid-infrared QCL. According to the mechanism of active mode locking of terahertz QCLs [23], if the fundamental and high-order RF signals are injected into the QCL simultaneously, a very sharp temporal modulation could be realized (i.e., an ultrashort electrical pulse). This would rapidly modulate the QCL gain, taking advantage of their ultrafast dynamics, permitting a small section of the cavity to be brought above the lasing threshold, while the rest of the active medium is held below threshold. This may permit the generation of ultrashort and intense light pulses from mid-infrared QCLs.

5. CONCLUSION

To conclude, we have demonstrated for the first time to our knowledge the injection locking and harmonic injection locking of a mid-infrared QCL with an output power over 1 W in CW operation at high temperature. Compared with an unlocked laser, the intermode spacing fluctuation of the injection-locked QCL emission has been considerably reduced by a factor beyond 1×10^3 , which enables demonstration of a highly stable

mid-infrared semiconductor laser with high phase coherence and high frequency purity. Despite an operating temperature change, the intermode spacing of laser emission is still stabilized to hertz level in the locking range by the external microwave modulation up to ~ 18 GHz. This result enables the practical applications of high-power, high-speed, highly stable QCLs in industrial exploration. It may also bring a revolution for next-generation optical communication and stimulate new concepts to explore ultrafast and intense mid-infrared pulse generation from QCL-based semiconductor sources.

Disclosures. The authors declare no conflicts of interest.

Data Availability. Data underlying the results presented in this paper are not publicly available at this time but may be obtained from the authors upon reasonable request.

REFERENCES

1. C. D. Nabors, A. D. Farinas, T. Day, S. T. Yang, E. K. Gustafson, and R. L. Byer, "Injection locking of a 13-W cw Nd:YAG ring laser," *Opt. Lett.* **14**, 1189–1191 (1989).
2. R. T. Ramos, A. J. Seeds, A. Bordonalli, P. Gallion, and D. Erasme, "Optical injection locking and phase-lock loop combined systems," *Opt. Lett.* **19**, 4–6 (1994).
3. A. E. Siegman, *Lasers* (University Science Books, 1986).
4. F. R. Ahmad and F. Rana, "Fundamental and subharmonic hybrid mode-locking of a high-power (220 mW) monolithic semiconductor laser," *IEEE Photon. Technol. Lett.* **20**, 1308–1310 (2008).
5. G. Fiol, D. Arsenijević, D. Bimberg, A. G. Vladimirov, M. Wolfrum, E. A. Viktorov, and P. Mandel, "Hybrid mode-locking in a 40 GHz monolithic quantum dot laser," *Appl. Phys. Lett.* **96**, 011104 (2010).
6. C. Ji, N. Chubun, R. G. Broeke, J. Cao, Y. Du, P. Bjeletich, and S. J. B. Yoo, "Electrical subharmonic hybrid mode locking of a colliding pulse mode-locked laser at 28 GHz," *IEEE Photon. Technol. Lett.* **17**, 1381–1383 (2005).
7. U. Keller, "Recent developments in compact ultrafast lasers," *Nature* **424**, 831–838 (2003).
8. G. E. Villanueva, M. Ferri, and P. Perez-Millan, "Active and passive mode-locked fiber lasers for high-speed high-resolution photonic analog-to-digital conversion," *IEEE J. Quantum Electron.* **48**, 1443–1452 (2012).
9. F. F. Voigt, F. Emaury, P. Bethge, D. Waldburger, S. M. Link, S. Carta, A. van der Bourg, F. Helmchen, and U. Keller, "Multiphoton *in vivo* imaging with a femtosecond semiconductor disk laser," *Biomed. Opt. Express* **8**, 3213–3231 (2017).
10. J. J. McFerran, "Échelle spectrograph calibration with a frequency comb based on a harmonically mode-locked fiber laser: a proposal," *Appl. Opt.* **48**, 2752–2759 (2009).
11. M. Razeghi, *The MOCVD Challenge: A Survey of GaInAsP-InP and GaInAsP-GaAs for Photonic and Electronic Device Applications*, 2nd ed. (CRC Press, 2017).
12. M. Razeghi, "High power, high wall-plug efficiency, high reliability, continuous-wave operation quantum cascade lasers at Center for Quantum Devices," *Proc. SPIE* **11296**, 112961C (2020).
13. F. Wang, V. Pistore, M. Riesch, H. Nong, P.-B. Vigneron, R. Colombelli, O. Parillaud, J. Mangeney, J. Tignon, C. Jirauschek, and S. S. Dhillon, "Ultrafast response of harmonic modelocked THz lasers," *Light Sci. Appl.* **9**, 51 (2020).
14. D. G. Revin, M. Hemingway, Y. Wang, J. W. Cockburn, and A. Belyanin, "Active mode locking of quantum cascade lasers in an external ring cavity," *Nat. Commun.* **7**, 11440 (2016).
15. J. Hillbrand, N. Opačak, M. Piccardo, H. Schneider, G. Strasser, F. Capasso, and B. Schwarz, "Mode-locked short pulses from an 8 μm wavelength semiconductor laser," *Nat. Commun.* **11**, 5788 (2020).
16. M. R. St-Jean, M. I. Amanti, A. Bernard, A. Calvar, A. Bismuto, E. Gini, M. Beck, J. Faist, H. C. Liu, and C. Sirtori, "Injection locking of mid-infrared quantum cascade laser at 14 GHz, by direct microwave modulation," *Laser Photon. Rev.* **8**, 443–449 (2014).
17. E. Rodríguez, A. Mottaghizadeh, D. Gacemi, M. Jeannin, Z. Aghari, A. Vasanelli, Y. Todorov, Q. J. Wang, and C. Sirtori, "Tunability of the free-spectral range by microwave injection into a mid-infrared quantum cascade laser," *Laser Photon. Rev.* **14**, 1900389 (2020).
18. W. Zhou, Q.-Y. Lu, D.-H. Wu, S. Slivken, and M. Razeghi, "High-power, continuous-wave, phase-locked quantum cascade laser arrays emitting at 8 μm ," *Opt. Express* **27**, 15776–15785 (2019).
19. Q. Lu, F. Wang, D. Wu, S. Slivken, and M. Razeghi, "Room temperature terahertz semiconductor frequency comb," *Nat. Commun.* **10**, 2403 (2019).
20. A. Hugi, G. Villares, S. Blaser, H. C. Liu, and J. Faist, "Mid-infrared frequency comb based on a quantum cascade laser," *Nature* **492**, 229–233 (2012).
21. Y. Dong, T. K. Johansen, and V. Zhurbenko, "Ultra-wideband coplanar waveguide-to-asymmetric coplanar stripline transition from DC to 165 GHz," *Int. J. Microw. Wireless Technol.* **10**, 870–876 (2018).
22. R. Adler, "A study of locking phenomena in oscillators," *Proc. IEEE* **61**, 1380–1385 (1973).
23. F. Wang, K. Maussang, S. Moumdji, R. Colombelli, J. R. Freeman, I. Kundu, L. Li, E. H. Linfield, A. G. Davies, J. Mangeney, J. Tignon, and S. S. Dhillon, "Generating ultrafast pulses of light from quantum cascade lasers," *Optica* **2**, 944–949 (2015).